

Tritium Particle Transport Experiments on TFTR during D-T Operation

P. C. Efthimion, L. C. Johnson, J. D. Strachan, E. J. Synakowski, M. Zarnstorff, H. Adler, C. Barnes,* R. V. Budny, F. C. Jobes, M. Louglin,† D. McCune, D. Mueller, A. T. Ramsey, G. Rewoldt, A. L. Roquemore, W. M. Tang, and G. Taylor

Plasma Physics Laboratory, Princeton University, Princeton, New Jersey 08543

(Received 7 December 1994)

The $t(d, n)\alpha$ and $d(d, n)^3\text{He}$ neutron emissivity profiles are measured in a deuterium neutral-beam–heated plasma where a small amount of tritium (T) gas has been puffed. The tritium density is inferred from the neutron emissivities, and transport coefficients (D, V) are determined. The particle diffusivities of T and ^4He and the thermal diffusivity are similar in magnitude and profile shape. The convective velocity is small for $r/a < 0.6$, and is anomalous for $r/a > 0.6$. These are the first measurements of D and V for a hydrogen isotope in a tokamak plasma.

PACS numbers: 52.55.Fa, 52.25.Fi

An understanding of transport properties in confined plasmas is important to the design of a fusion reactor. It is well established that neoclassical theory, which deals only with classical collisional processes, cannot account for the experimentally observed rates of plasma transport. The leading explanation is that collective (e.g., wave-particle interaction) dynamics driven by microinstabilities play a role in increasing transport losses, especially in the interior regions of the plasma where complications due to atomic physics and boundary conditions are not expected to be dominant [1]. The microinstabilities can be electrostatic or magnetic in nature, and can affect both the particle and heat transport. In the area of particle transport, the first experiments were on the T-3 tokamak, where changes in the electron density due to a small gas puff were measured with interferometry [2]. Similar studies were completed on many tokamaks with interferometry and Thomson scattering measuring the electron density [3–6]. Ion transport studies have relied on spectroscopic measurements of high- Z impurity elements, including iron, germanium, and selenium [7,8]. Recent developments in charge-exchange recombination spectroscopy diagnostics have provided a means of studying fully stripped low- Z elements such as helium and carbon [9,10]. However, the measurement of hydrogenic ion transport has remained elusive, because no spectroscopic technique has been identified with sufficient accuracy to measure the local ion density. Fusion product techniques were used to study ^3He transport with limited spatial resolution, and a similar approach was proposed to infer the trace tritium density in a deuterium plasma from the 14.1 MeV $t(d, n)\alpha$ and 2.5 MeV $d(d, n)^3\text{He}$ neutron emissivities [11,12]. In the tritium beam experiments on JET, the local 14.1 MeV $t(d, n)\alpha$ and 2.5 MeV $d(d, n)^3\text{He}$ neutron emissivity profiles have been measured, and the transport using various mixing models to predict the local evolution of tritium and deuterium was studied with the global introduction of tritium by neutral beam injection [13,14].

In November 1993, TFTR started tritium operation to explore tritium and alpha particle physics [15,16]. This paper reports the results of tritium transport studies where small amounts of tritium gas were puffed into deuterium neutral-beam–fueled plasmas. The local 14.1 MeV $t(d, n)\alpha$ and 2.5 MeV $d(d, n)^3\text{He}$ neutron emissivity profiles were measured, and the ion density profile was inferred [17]. The introduction of the tritium in the form of a small gas puff allows for the application of trace transport analysis techniques to ascertain the local transport coefficients [6,18]. These results represent the first measurement of hydrogenic ion transport coefficients in the form of a diffusivity and convective velocity (D_T, V_T) in a tokamak plasma. Measurement of hydrogenic ion transport is fundamental to understanding the physics of plasma transport. Furthermore, characterization of local ion transport is important to future reactors, such as ITER, because transport directly impacts reactor density profile control [19,20]. Density profile control may provide operational flexibility to meet the requirements of stable core fusion power production and edge density control to avoid disruptions, remove helium ash, and limit impurities.

The experiment examined tritium transport in high performance, low recycling, deuterium neutral-beam–fueled plasmas, referred to as supershots. The specific device parameters were the same as previously studied for electron, ^4He , and impurity transport [21]. The neutral beams were injected into a deuterium plasma countertangential and contangential to the plasma current, with a maximum energy ≈ 100 keV and 14 MW of power. The tokamak operating parameters included a toroidal magnetic field of $B_\phi = 4.8$ T, a major radius of $R = 2.45$ m, a minor radius of $a = 0.8$ m, and a plasma current of $I_p = 1.15$ MA. The central electron and ion temperatures were $T_e(0) \approx 7.5$ keV and $T_i(0) \approx 25$ keV, respectively, and the central electron density was $n_e(0) \approx 5 \times 10^{19} \text{ m}^{-3}$. The Z_{eff} profile was hollow with a value of 2.1 at the plasma center and 3.8 near the edge. The global energy confinement time for this plasma

was 0.16 s, which is approximately 3 times the ITETP89 *L*-mode confinement scaling [22]. Figure 1 shows the time evolution of the line-integrated electron density and the total neutron source strength. The deuterium neutral beams were injected from 3 to 4 s. A tritium puff of gas (≈ 3 torr liter/s for 0.016 s) was applied at 3.5 s and resulted in a large change in the total neutron source strength. This was the only gas puff size used in this experiment. The neutron source strength for a comparable plasma with no tritium gas puff is represented by the dotted line in the neutron wave form. The ratio of central tritium to deuterium density rises from ≈ 0.001 before 3.5 s to ≈ 0.01 due to the gas puff as estimated by the ratio of 14.1 MeV $t(d,n)\alpha$ and 2.5 MeV $d(d,n)^3\text{He}$ neutron emissivities. Thus, tritium is an ideal gas to use in trace transport experiments because a small quantity of gas yields a large diagnostic response.

The main diagnostics on TFTR for tritium studies are three collimated neutron systems: a 5 channel ^4He proportional counter array that is sensitive only to the 14.1 MeV $t(d,n)\alpha$ neutrons, a 10 channel NE-451 ZnS detector array that is sensitive to both the 14.1 MeV $t(d,n)\alpha$ and 2.5 MeV $d(d,n)^3\text{He}$ neutrons, and a second 10 channel array with less sensitive ZnS wafer scintillators [23,24]. The proportional counters and the NE-451 scintillators were absolutely calibrated *in situ* using a D-T neutron generator [25,26]. The ZnS detector arrays with 10 vertical sight lines are particularly useful in obtaining local transport information. Figure 2 shows the time evolution of the local 14.1 MeV $t(d,n)\alpha$ neutron emissivity profile after the injection of the tritium gas puff near 3.5 s, as measured by the ZnS detector array. The 14.1 MeV $t(d,n)\alpha$ neutron emissivity is determined from the total chordal neutron measurement by subtracting the 2.5 MeV $d(d,n)^3\text{He}$ neutron contribution measured in similar deuterium plasma discharges, and Abel inverting the resulting chordal neutron profile. Statistical accuracy was improved by averaging 5 shots with tritium gas puffs while averaging 4 of the equivalent shots with deuterium gas puffs. In Fig. 2 the local neutron emissivity due to the tritium gas puff starts out hollow and quickly peaks up within 0.05 s. The hollow

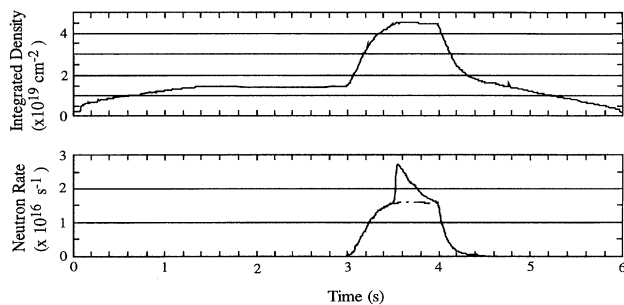


FIG. 1. Evolution of the integrated density and the total neutron reaction rate for a deuterium neutral beam plasma with a gas puff near 3.5 s. For the neutron wave form the reaction rates for a tritium (solid line) and deuterium (dotted line) are compared.

neutron emissivity profile is indicative of a hollow tritium density at the early times of its evolution.

Nuclear techniques for measuring plasma ion density have been described by Strachan *et al.* [11,12]. The techniques rely upon the majority of the neutrons originating from beam-thermal reactions:

$$I_{dd} \approx n_d \xi \dot{N}_B \tau_{dd} \langle \sigma V \rangle_{dd}, \quad (1)$$

$$I_{dt} \approx n_t \xi \dot{N}_B \tau_{dt} \langle \sigma V \rangle_{dt}, \quad (2)$$

where I_{dt} and I_{dd} are the 14.1 MeV $t(d,n)\alpha$ and 2.5 MeV $d(d,n)^3\text{He}$ neutron reaction rates, n_d and n_t are the deuterium and tritium densities, ξ is the percentage of the full energy component of the neutral beam which is centrally trapped and confined on its first ion orbits, \dot{N}_B is the injection rate of the full energy component ions, τ_{dd} and τ_{dt} are the cross-section weighted slowing down times of the full energy component ions, and $\langle \sigma V \rangle_{dd}$ and $\langle \sigma V \rangle_{dt}$ are the respective average cross sections. However, the ratios of the reaction rates are primarily sensitive to n_d and n_t , and only weakly to the ion temperature (T_i) in keV: $I_{dt}/I_{dd} \approx (n_t/n_d) 67.3 \exp(0.72/T_i^{0.33})$.

These techniques assume that the neutrons are all from beam-thermal reactions. However, in the supershot studied here, $\approx 65\%$ of the 2.5 MeV $d(d,n)^3\text{He}$ neutrons are from beam-thermal reactions and the remainder are thermal and beam-beam reactions. Furthermore, only 50% of the central 2.5 MeV $d(d,n)^3\text{He}$ neutrons are from beam-thermal reactions. To take the thermal contribution into account, a new constant can be applied to the ratio of the neutron reaction rates. Here, an alternate algorithm was developed to infer the ion density profile. A response function, similar to a Green's function, is calculated, relating the tritium ion density, $n_t(r,t)$, to the measured 14.1 MeV $t(d,n)\alpha$ neutron emissivity for this plasma discharge, $S_{dt}(r,t)$. The analysis code TRANSP [27], using the measured plasma density, temperatures,

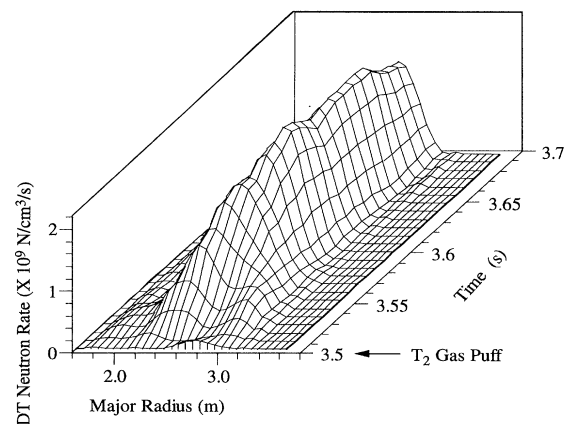


FIG. 2. Local 14.1 MeV $t(d,n)\alpha$ neutron emissivity profile due to the pure tritium gas puff starting at 3.5 s. The emissivity profile starts out hollow and rapidly reaches a peak.

Z_{eff} , magnetics, and the neutral beam injection parameters, computes the local 14.1 MeV $t(d,n)\alpha$ neutron emissivity, $S_{dt}^*(r,t)$, for a constant amount of tritium density, $n_t^* = 5 \times 10^{17} \text{ m}^{-3}$, at each plasma radius and for all time. This represents the 14.1 MeV $t(d,n)\alpha$ neutron response for a fixed amount of tritium for the plasma including both beam-thermal and thermal reactions. Then the tritium density, $n_t(r,t)$, can be estimated from the measured 14.1 MeV $t(d,n)\alpha$ neutron measurement $S_{dt}(r,t)$ according to the simple relation

$$n_t(r,t) \approx n_t^*[S_{dt}(r,t)]/S_{dt}^*(r,t). \quad (3)$$

The response function is merely $n_t^*/S_{dt}^*(r,t)$, and it has a range of values of 28 to 1×10^5 . The time evolution of the tritium density profile inferred by this technique for the neutron emissivity profile in Fig. 2 is shown in Fig. 3. The profile starts out hollow, fills in as tritium diffuses into the core, and reaches a slightly peaked shape in ≈ 0.1 s. This behavior is similar to that of the electrons, previously measured on TFTR [6]. Note that the peak of the profile is near $R = 2.7$ m, which is consistent with the position of the magnetic axis. The profile shape is somewhat less peaked than the electron density profile, and the helium and carbon profiles measured with charge-exchange recombination spectroscopy [9,10]. The peakedness of tritium profile, $n(0)/\langle n \rangle$, at 3.63 s is 1.9, while it is 2.3 for the electron profile. The differences in the profile shapes can be partly attributed to the limited spatial resolution of the neutrons in the core of the plasma and a 15% uncertainty in the neutron calibration.

The time-dependent density profile and the gas puff source are used in the TRANSP analysis code to calculate the tritium particle flux, $\Gamma(r,t)$, from the particle balance equation: $\partial n/\partial t = -\nabla \cdot \Gamma + S$, where S is the tritium

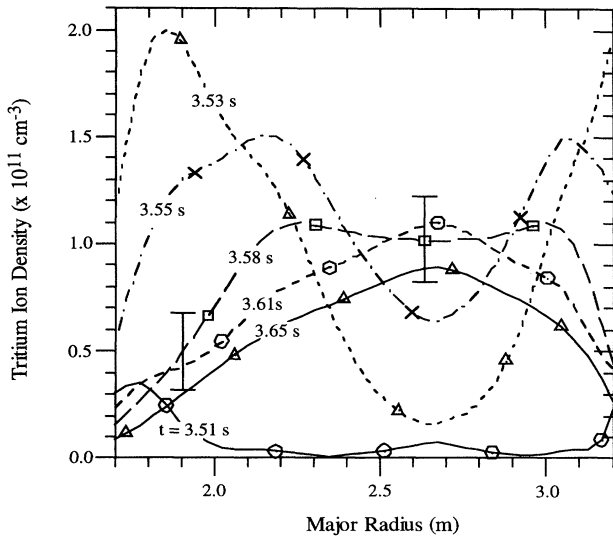


FIG. 3. Evolution of tritium density profile inferred from the neutron emissivity profiles for a pure tritium gas puff. The tritium profile starts out hollow and fills in ≈ 0.01 s, showing diffusive transport.

source. Then at each radius, r , a regression analysis of the particle flux is used to determine the transport coefficients according to the relationship

$$\Gamma(r,t) = -D_T(r)\nabla n(r,t) + V_T(r)n(r,t), \quad (4)$$

where $D_T(r)$ and $V_T(r)$ are the local tritium transport coefficients. The same techniques have been used in the study of electron particle transport [6,18]. The tritium perturbation is considered a trace because the central tritium density after injection is $\approx 1\%$ of the deuterium density and the residual amount of tritium density prior to the gas puff is $\approx 0.1\%$. In this experiment the neutron detectors averaged counts for 0.008 s, which limited the time resolution of the data analysis. This is an issue in the analysis of the outer plasma radii where the duration of the local density perturbation is only 0.04 s. The limited number of data points is responsible for higher uncertainty in the convective velocity, V_T , at the outer radii.

Figure 4 shows the tritium transport coefficients, $D_T(r)$ and $V_T(r)$, as determined from multiple regression analysis. In addition, the transport coefficients of ^4He measured by charge-exchange recombination spectroscopy on similar plasma discharges are shown for comparison [21]. Also included in the plot is the deuterium thermal conductivity determined from equilibrium power balance analysis. The three diffusivities are similar in magnitude and profile shape: $D_T \approx D_{\text{He}} \approx \chi_D$. The similarity of the

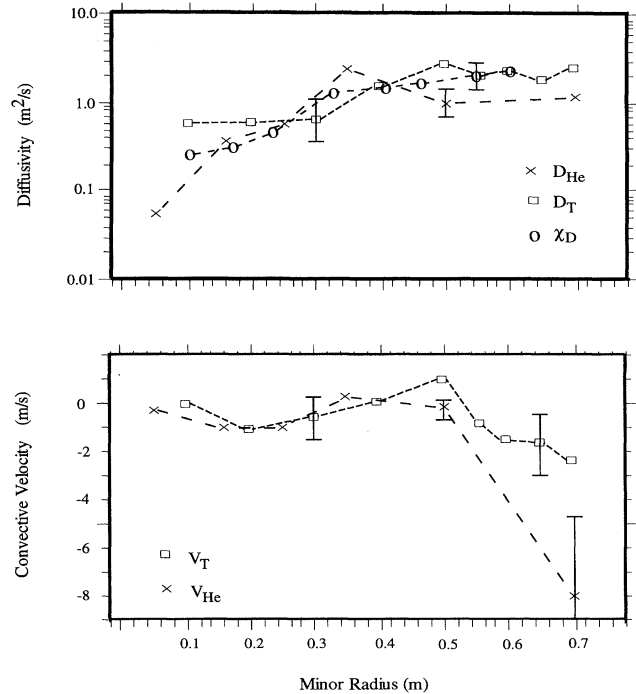


FIG. 4. Comparison of tritium and helium particle diffusivities and convective velocities. Also included is the thermal diffusivity. The diffusivities of tritium, helium, and heat are of similar magnitudes.

particle and heat diffusivities has been observed in previous perturbative transport experiments on TFTR and is a prominent characteristic of transport due to driftlike microinstabilities [6,10,21]. In addition, the similarity in the diffusivities is attractive with regard to helium ash buildup for future reactors, such as ITER [21]. There is an inward pinch in the tritium transport coefficients with values large compared to neoclassical theory for $r > 0.5$ m. The tritium pinch velocities are very low, being within error bars of zero for $r < 0.5$ m. The expected neoclassical pinch is also small (≈ 0.04 m/s). The chordal neutron data can be simulated with the measured diffusivities, the measured pinch values for $r > 0.5$ m, and neoclassical values for $r < 0.5$ m. Therefore, the measured tritium pinch is consistent with neoclassical values for $r < 0.5$ m, but the error bars do not allow us to conclude that it is not anomalous. It is difficult to compare these results with previous measurements of the electron convective velocity (≈ 1 m/s), because the electrons are not a trace perturbation and the velocity has contributions from the inward pinch and nonlinearities in the diffusivity [e.g., $D = F(n, \nabla n)$] [6,21]. The error bars in the figures were obtained by propagating the uncertainty in the neutron data through the entire analysis: Abel inversion, TRANSP analysis, and regression analysis.

A quasilinear transport model, predominantly due to enhanced $\mathbf{E} \times \mathbf{B}$ drift by plasma microinstabilities, has been applied to the present experimental data [28]. The associated theory of turbulent transport in toroidal plasmas is a complex and evolving subject. The quasilinear transport model is a well known approach involving the utilization of a fully kinetic model in which all relevant linear and quasilinear physics properties are self-consistently taken into account. However, simplified mixing-length estimates from strong turbulence theory need to be invoked for the saturation amplitude of the fluctuations. While this model is not definitive, applications of this type of approach to analyze and interpret transport trends have been encouraging [21]. The eigenmodes and eigenfrequencies of electrostatic and electromagnetic modes were calculated in toroidal geometry. The profiles of the electron and ion temperatures, electron density, carbon density, and Z_{eff} were used in the quasilinear calculation. The beam ion energy distribution and ion density as calculated by TRANSP were used. The ratio of V/D was calculated at $r/a = 0.2$ and 0.5 for the ion species D, T, and ^4He . These ratios are compared to the present tritium and the previous ^4He results [21]. At $r/a = 0.2$ there is good agreement between the model and measurements: the model estimates $V/D \approx -2.4 \text{ m}^{-1}$ for ^4He , $V/D \approx -3.2 \text{ m}^{-1}$ for tritium, and $D_T/\chi \approx 1.2$ while the experimental values are $V/D \approx -2.6 \text{ m}^{-1}$ for ^4He , $V/D \approx -1.6 \pm 0.5 \text{ m}^{-1}$ for tritium, and $D_T/\chi \approx 1.5 \pm 0.8$. At $r/a = 0.5$ the model estimates $V/D \approx -2.6 \text{ m}^{-1}$ for ^4He , $V/D \approx -1.4 \text{ m}^{-1}$ for tritium, and $D_T/\chi \approx 7.4$ while the experimental values are $V/D \approx -2.6 \text{ m}^{-1}$ for ^4He , $V/D \approx 0.2 \pm 0.4 \text{ m}^{-1}$

for tritium, and $D_T/\chi = 1.2 \pm 0.6$. There are disagreements in the ratio of V/D for tritium and D_T/χ at $r/a = 0.5$. The model is sensitive to the local ion density gradients which are experimentally determined from the electron density profile and the carbon profile, the main impurity in these plasmas. For example, the model predicts ratios of the transport coefficients changing a factor of 2 when the ion density is inferred assuming a flat Z_{eff} profile instead of the nonuniform impurity profile.

We wish to acknowledge the contributions to this work from the Princeton Plasma Physics Laboratory technical and engineer personnel under the leadership of R. Davidson. This work was supported by DOE Contract No. DE-AC02-76CH03073.

*Permanent address: Los Alamos National Laboratories, Los Alamos, New Mexico 87545

†Permanent address: Joint European Undertaking, United Kingdom.

- [1] J. D. Callen *et al.*, Phys. Fluids B **2**, 2869–2960 (1990).
- [2] A. V. Berlizov *et al.*, in *Plasma Physics and Controlled Nuclear Fusion Research 1980, Brussels* (IAEA, Vienna, 1981), Vol. 1, p. 23.
- [3] J. D. Strachan *et al.*, Nucl. Fusion **22**, 1145 (1982).
- [4] K. W. Gentle *et al.*, Plasma Phys. Controlled Fusion **29**, 1077 (1987).
- [5] N. L. Vasin *et al.*, Sov. J. Plasma Phys. **10**, 525 (1984).
- [6] P. C. Efthimion *et al.*, Phys. Rev. Lett. **66**, 421 (1991).
- [7] B. C. Stratton *et al.*, Nucl. Fusion **31**, 171 (1991).
- [8] E. S. Marmor *et al.*, Nucl. Fusion **22**, 1567 (1982).
- [9] R. J. Fonck and R. A. Hulse, Phys. Rev. Lett. **52**, 530 (1984).
- [10] E. J. Synakowski *et al.*, Phys. Rev. Lett. **65**, 2255 (1990).
- [11] J. D. Strachan *et al.*, J. Vac. Sci. Technol. A **1**, 811 (1983).
- [12] J. D. Strachan and A. Chan, Nucl. Fusion **27**, 1025 (1987).
- [13] F. B. Marcus *et al.*, Nucl. Fusion **33**, 1325 (1993).
- [14] B. Balet *et al.*, Nucl. Fusion **33**, 1345 (1993).
- [15] R. Hawryluk *et al.*, Phys. Rev. Lett. **72**, 3530 (1994).
- [16] J. D. Strachan *et al.*, Phys. Rev. Lett. **72**, 3526 (1994).
- [17] L. C. Johnson *et al.*, in Proceedings of the 21st European Conference, Montpellier, 1994 (European Physical Society, Petit-Lancy, to be published).
- [18] P. C. Efthimion *et al.*, in *Plasma Physics and Controlled Nuclear Fusion Research 1988, Nice, France* (IAEA, Vienna, 1989), Vol. 1, pp. 307–321.
- [19] W. Houlberg *et al.*, Nucl. Fusion **34**, 93 (1994).
- [20] K. Borrass *et al.*, in *Plasma Physics and Controlled Nuclear Fusion Research 1990, Washington, D.C.* (IAEA, Vienna, 1991), Vol. 3, p. 343.
- [21] E. J. Synakowski *et al.*, Phys. Fluids B **5**, 2215 (1993).
- [22] P. N. Yushmanov *et al.*, Nucl. Fusion **30**, 1999 (1990).
- [23] L. C. Johnson, Rev. Sci. Instrum. **63**, 4517 (1992).
- [24] A. L. Roquemore *et al.*, Rev. Sci. Instrum. **66**, 916 (1994).
- [25] J. Strachan, Rev. Sci. Instrum. **66**, 1247 (1994).
- [26] D. L. Jassby *et al.*, Rev. Sci. Instrum. **66**, 891 (1994).
- [27] R. J. Hawryluk *et al.*, in *Physics Close to Thermonuclear Conditions, Varenna, Italy, 1979* (Commission of the European Communities, Brussels, 1979).
- [28] G. Rewoldt and W. M. Tang, Phys. Fluids B **2**, 318 (1990).